Bioresource Technology 413 (2024) 131516

Contents lists available at ScienceDirect

Bioresource Technology

journal homepage: www.elsevier.com/locate/biortech

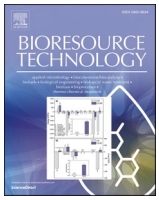

Exploring different processes for starch extraction from microalgae and synthesis of starch-chitosan plastic films

Fabrizio Di Caprio *, Nooshin Pedram, Benedetta Brugnoli, Iolanda Francolini, Pietro Altimari, Francesca Pagnanelli

Department of Chemistry, University Sapienza of Rome, Piazzale Aldo Moro 5, 00185 Rome, Italy

HIGHLIGHTS

- New process configurations to refine microalgal starch are described.
- Alcalase allows starch refining up to 58 % along with protein hydrolysate extraction.
- Sonication in DMSO and starch precipitation in ethanol allows starch purification.
- Up to 91 % starch purity and 80 % extraction recovery attained with DMSO extraction.
- Chitosan-starch films were produced with purified algal starch and defatted algae.

ARTICLE INFO

Keywords:
Tetradesmus obliquus
Bioplastic
Enzymatic treatment
Biorefinery
Protease
Thermoplastic starch

ABSTRACT

Microalgae could become a more sustainable starch source than conventional crops. However, available refinery processes are lacking. In this study, we develop different innovative processes to refine microalgal starch and obtaining starch-based bioplastics. After lipid extraction, defatted microalgae were treated by different routes: enzymatic treatment with Alcalase; sonication in hot water or dimethyl sulfoxide (DMSO) followed by precipitation with ethanol.

Enzymes allows to extract 70 % of proteins while recovering 75 % of the initial starch in the residual pellet, with a purity of 58 %. The most effective configuration based on sonication and water/DMSO extraction allowed to recover up to 80 % starch with 80–91 % purity.

Chitosan improved the mechanical properties of the obtained starch-based films. The use of defatted algae or purified starch gave different properties to the films (as rigidity and water stability) showing the possibility to tailor the material characteristics depending on the biorefinery route applied.

1. Introduction

Starch is a biodegradable biopolymer with diverse applications in sectors such as food production, food additives, and bio-based materials. The worldwide production has been estimated between 88–98 million tons per year in 2020 (Vilpoux and Santos Silveira Junior, 2023). This starch is primarily sourced from terrestrial crops like corn (75 %), cassava (14 %), wheat (7 %) and potatoes (4 %) (Vilpoux and Santos Silveira Junior, 2023). Microalgae represent a promising alternative source of starch. They can achieve starch productivities per hectare up to ten times higher than terrestrial plants (Gifuni et al., 2017), requiring significantly less water, and including the use of wastewaters or saltwater as a water source (Wang et al., 2016). Additionally, microalgae can use fertilizers more efficiently than terrestrial plants, with yields close to 100 % (Wang et al., 2016; Zhang et al., 2015). Taken together, these characteristics position microalgae as a promising future alternative for starch production, potentially with lower environmental impacts compared to conventional crops.

In addition to starch, microalgae can serve as a source of other biomolecules, including lipids as triglycerides (TAGs), pigments and proteins with biological value comparable to eggs and meat (Fernández et al., 2021). Currently, microalgae industry predominantly focuses on single products such as dry biomass, pigments (astaxanthin, phycocyanin), and omega-3 fatty acids, intended for use as food and feed

* Corresponding author.
E-mail address: fabrizio.dicaprio@uniroma1.it (F. Di Caprio).

https://doi.org/10.1016/j.biortech.2024.131516
Received 16 July 2024; Received in revised form 10 September 2024; Accepted 20 September 2024
Available online 21 September 2024

additives (Araújo et al., 2021). Implementing a biorefinery process could enable the valorization of various biomass components, including starch (Nitsos et al., 2020). Nevertheless, the potential for integrating lipid and protein extraction with starch recovery has been largely overlooked. A primary technical challenge in starch purification lies in its insolubility in many common solvents. Native starch can be refined only as result of the removal of non-starch components, such as lipids, proteins, and other cellular components (do Carmo Cesário et al., 2022), by their selective extraction. This is the approach employed by conventional processes for extracting starch from terrestrial plants sources: mechanical cell disruption followed by protein separation in a water suspension (El Halal et al., 2019). However, this kind of process is difficult to be applied to microalgae due to their smaller cell size, smaller starch granule size, and lower starch content (≤45 % compared to 80–85 % for terrestrial plants)(Alhattab et al., 2019; Nitsos et al., 2020). In previous studies, microalgal starch has been purified using cell disruption methods followed by centrifugation through a Percoll gradient (Gifuni et al., 2017; Izumo et al., 2007). However, Percoll gradient is hardly applicable at industrial scale. Recently, cell disruption followed by aqueous two-phases systems (ATPS) and ethanol extraction have been reported as promising methods to separate microalgal starch from other cellular components (Di Caprio et al., 2022; Suarez Ruiz et al., 2020b, 2020a). However, the reported purity of refined starch obtained with these approaches was not higher than 56 %. Previous approaches were based on conditions that prevented starch gelatinization, to recover it in the native form. The limitations in the final purity attained suggest that achieving higher purity with such an approach may not be feasible. The main limit of such an approach is the presence of other insoluble components, mainly empty cell walls (made of proteins, cellulose and sporopollenin) (do Carmo Cesário et al., 2022), that can remain in the insoluble fraction along with native starch.

The aim of this study is to overcome these previous issues by testing and comparing different innovative approaches for refining microalgal starch: i) an enzymatic treatment of defatted biomass, to selectively separate proteins from starch after lipid extraction; ii) a starch extraction from defatted biomass by its solubilization in hot water or dimethyl sulfoxide (DMSO), followed by starch precipitation with ethanol. Finally, for the first time, a plastic-film composed by a blend of microalgal starch and chitosan has been synthetized and assessed for its mechanical and physical properties.

2. Materials and methods

2.1. Microalgae cultivation

A non-axenic strain of *Tetradesmus obliquus* was isolated as previously described (Di Caprio et al., 2022), and cultivated in two 500 mL column glass photobioreactors (PBRs) (h = 35 cm, d = 5 cm), at an initial concentration of 0.3 g L^{-1}. The temperature was maintained at 28 ± 1 °C and pH was kept at 7.5 ± 0.5 (controlled by CO_2 supply). The PBRs were illuminated 24 h/d using LED light lamps (GROWSTAR L-QB1), providing 500 ± 50 μmol s^{-1} m^{-2} photons (measured by a luxmeter at three different heights; conversion factor: 0.0257). Each PBR was fed with 1 L min^{-1} air (filtered at 0.2 μm) and 10 mL min^{-1} of pure CO_2. Modified M8 medium was used as culture medium (see supplementary material). To generate sufficient biomass, various cultivation batches were repeated. The biomass was harvested at concentrations ranging between 4–8 g L^{-1}, following the guidelines previously described to enhance starch accumulation by exploiting N-starvation (Di Caprio et al., 2023). The biomass was harvested by centrifugation (3000g x 10 min), then suspended in distilled water aliquots at 90 g L^{-1}, and finally frozen at − 18 °C until its utilization for the experiments. The dry weight of microalgae suspensions was determined by filtering samples through 0.7 μm glass fiber filters and then oven dried at 105 °C before weighing.

2.2. Lipid extraction on fresh biomass

Defrosted wet biomass was centrifuged to remove residual water and suspended in pure ethanol (99 %) at a ratio of 10 mL solvent per 1 g of dry biomass equivalent. This suspension was transferred into 50 mL glass reactors, under magnetic stirring, heated at the boiling temperature of ethanol. After 15 min, the suspension was centrifuged (3000g x 5 min), the solvent removed, and the pellet was suspended again in ethanol for a new extraction cycle. The procedure was repeated for 9 extraction cycles, and the residual pellet was dried at 105 °C, finally ground, and then stored.

2.3. Enzymatic treatment with Alcalase for protein extraction

After extracting lipids from the wet biomass, the resulting defatted biomass was used for enzymatic protein extraction tests. For each test, 600 mg of dry defatted biomass was suspended in 30 mL buffer solution (93.5 mM K_2HPO_4, 6.5 mM KH_2PO_4, pH 8.0) in a 50 mL reactor (h = 11.4 cm, d = 3.5 cm) maintained at a constant temperature using a water jacket connected to a thermocryostat (CB5-10, Giorgio Bormac srl, Modena, Italy). The biomass suspension underwent magnetic stirring for 30 min to achieve a homogenous suspension and a constant temperature. The extraction process was started by adding 0.3 mL of an enzymatic solution containing the *endo*-peptidase Alcalase from *Bacillus licheniformis* (≥0.75 Anson units mL^{-1}, cod. 126741, Merck). The extraction was carried out at 30 °C, 40 °C and 50 °C for 6 h. After 6 h, the residual pellet was harvested by centrifugation (7000g x 5 min), washed twice with distilled water, and finally dried overnight in the fume hood. These extractions were performed in duplicate, and negative control tests without enzyme were conducted for each temperature. The biomass recovery was calculated by eq. (1):

$$Y_x = \frac{m_{x,f}}{m_{x,0}} \tag{1}$$

With $m_{X,0}$ and $m_{X,f}$ the initial and final biomass respectively.

The protein extraction efficiency (Y_P) was quantified by eq. (2):

$$Y_P = \frac{\left(C_N(t) - C_{N,0}\right)V}{m_{x,0}X_{N,0}} \tag{2}$$

with $C_N(t)$ the nitrogen concentration in the liquid phase at extraction time *t*, $C_{N,0}$ the nitrogen concentration measured at t = 0 (nitrogen contribution by Alcalase), V the volume of the suspension, and $X_{N,0}$ the nitrogen content in the defatted biomass. The calculation assumes that released N is proportional to proteins.

$X_{N,0}$ was measured by a CNHS analysis carried out by an elemental analyzer (EA 1110 CHNS/O).

The starch extraction recovery in the residual pellet (Y_{starch}) was quantified by eq. (3):

$$Y_{starch} = \frac{X_{st,f}m_{x,f}}{X_{st,0}m_{x,0}} \tag{3}$$

With $X_{st,f}$ the starch content in the final biomass after treatment and $X_{st,0}$ the starch content in the initial defatted biomass.

2.4. Sonication pre-treatments of raw biomass in different solvents under different temperatures

Microalgae aliquots were thawed and suspended at 90 g L^{-1} in either 20 mL of water or ethanol (96 %) for sonication. The suspensions were placed in a 50 mL jacketed glass chamber (h = 5 cm; d = 4.4 cm). Sonication was performed using a Branson 450 Digital Sonifier (20 kHz, 400 W maximum output power) with a 12 mm replaceable probe immersed inside, operated in pulsed mode (t_{on} = 0.3 s, t_{off} = 0.1 s), at 60 % amplitude (90 μm) for a total treatment time (T) of 240 min. For both

ethanol and water as solvents, three different temperatures were tested:

- No temperature control. Sonication was carried out without any water recirculation in the jacket of the sonication chamber.
- Temperature control at 5 °C. Recirculating water at 5 °C in the jacket of the sonication chamber.
- Temperature control at 40 °C. Recirculating water at 40 °C in the jacket of the sonication chamber.

To prevent errors due to solvent evaporation, solvent was added to the chamber to restore the original volume before collecting samples, when required. Cell disruption efficiency of the sonication treatments was determined by measuring cell concentration at various time intervals using optical counting in a Thoma chamber and an optical microscope. The disruption efficiency was then calculated using Eq. (4):

$$\text{Cell disruption}\,(\%) = \frac{C_0 - C(T_{on})}{C_0}\,100 \quad (4)$$

With C_0 and $C(T_{on})$, the initial cell concentration and the concentration measured after a certain treatment time $T_{on} = T\frac{t_{on}}{t_{on}+t_{off}}$.

At the end of the sonication treatment, 1.5 mL sample aliquot was collected and centrifuged (7000g x 5 min). The resulting pellet was washed once with water, frozen at − 18 °C, and subsequently spray-dried (Labogene CoolSafe 55–4 PRO). The pellet was then analyzed for starch and total carbohydrate content, and the recovery calculated using Eq. (3). Total carbohydrates in the supernatant were also analyzed to quantify the fraction dissolved in the liquid phase during the treatment.

Simultaneously, another 10 mL aliquot was collected from each sample after sonication and centrifuged (3000g x 5 min). The resulting pellet was suspended in 10 mL of ethanol (96 %), and the tube was heated in a heat block at 100 °C for 15 min. After centrifugation, the solvent was separated, and ethanol was added again for a new extraction cycle. This procedure was repeated until the solvent remained transparent. Finally, the residual pellets were spray-dried and starch and carbohydrate content were analyzed once more. The recovery was calculated again using Eq. (3). These experiments were conducted in duplicate.

2.5. Starch extraction with DMSO and boiling water from defatted biomass

The extraction of starch from the defatted biomass was conducted under various conditions, as follows:

- D1. Defatted biomass was placed at 2 mg mL^{-1} in DMSO at 80 °C in a block for 90 min.
- D2. Defatted biomass was placed at 2 mg mL^{-1} in DMSO at 100 °C in a block for 90 min.
- W1. Defatted biomass was placed at 2 mg mL^{-1} in pure H_2O at 100 °C in a block for 90 min.
- D3. Defatted biomass was placed at 2 mg mL^{-1} in DMSO, and a 20 mL suspension was subjected to sonication (Branson 450 Digital Sonifier, 20 kHz, 400 W maximum output power) in a 50 mL jacketed glass chamber (h = 5 cm; d = 4.4 cm), with a 12 mm ultrasonic probe immersed inside. The sonication was carried out in pulsed mode (t_{on} = 0.1 s, t_{off} = 0.4 s), at 60 % amplitude (90 μm) for a total time (t_{on} + t_{off}) of 60 min.
- W2. Defatted biomass was placed at 2 mg mL^{-1} in water, and a 20 mL suspension was subjected to sonication, which was performed in the same conditions as D3, but with t_{on} = 0.1 s, t_{off} = 0.2 s.
- Kinetic test. For this test, the conditions of the test "W1", "W2" and "W1 + magnetic stirring" have been carried out for an extraction time of 240 min, and the supernatant (after centrifugation) was analyzed at different sampling times for total carbohydrate concentration.
- Effect of biomass concentration. The condition W1 was tested for three different defatted biomass concentrations: 0.5, 2, 8 and 20 mg mL^{-1}; for a treatment time of 240 min.

After extraction, all samples were centrifuged (3000g x 10 min) and 1 mL of the supernatant was transferred into a new tube. Then, 3 mL of pure ethanol were added to obtain starch precipitation. The sample was centrifuged again (3000g x 10 min) and the resulting pellet was analyzed to quantify starch extraction recovery and purity. These extractions were conducted in duplicate.

2.6. Starch extraction with DMSO and boiling water from pellet after sonication

The extraction of starch was also tested for all the different samples obtained after the raw biomass underwent sonication pre-treatment in water or ethanol, at various temperatures, as described in section 2.4, followed by defatting with ethanol. These different pre-treatments resulted in six different samples, replicate in duplicate. The pellets of these samples were spray-dried and then tested for starch extraction with the following procedures:

- Samples were placed at 2 mg mL^{-1} in DMSO at 100 °C in a block heater for 90 min.
- Samples were placed at 2 mg mL^{-1} in pure H_2O at 100 °C in a block heater for 90 min.

After extraction, all samples were centrifuged (4000 rpm x 10 min) and 1 mL of the supernatant was transferred into a new tube. Subsequently, 3 mL of pure ethanol were added to induce starch precipitation. The sample was centrifuged again (5000 rpm x 10 min) and the resulting pellet was analyzed to determine starch extraction recovery. These extractions were conducted in duplicate.

2.7. Chemical analysis

The starch content inside samples was measured by enzymatic hydrolysis by using the "total starch assay kit" (Megazyme, ref. K-TSTA, Ireland), following the protocol previously described (Di Caprio et al., 2022). Total carbohydrate content inside biomass samples was quantified by acid saccharification followed by spectrophotometric determination of sugars with the phenol–sulfuric acid method (Di Caprio et al., 2023). It should be noted that, as carbohydrates inside cells are almost exclusively made of polysaccharides, even the "total carbohydrates" value was obtained by multiplying for 0.9 factor, as for total starch, to account for water incorporated during the hydrolysis. Total nitrogen (TN) was analyzed by using the method for water analyses described by IRSA-CNR 4060 (Di Caprio et al., 2021b), based on the oxidation of organic nitrogen to nitrate followed by spectrophotometric analysis. Fourier Transform Infrared Spectroscopy was carried out using a FTIR model Nicolet 6700 (Thermo Fisher Scientific, Waltham, MA, USA) equipped with a Golden Gate ATR accessory (angle of incidence 45°). Spectra were recorded at 200 scans and a spectral resolution of 4 cm^{-1}. Absorbance was normalized with respect to the peak at 995 cm^{-1} corresponding to the C-OH stretching (Tedeschi et al., 2021).

2.8. Synthesis and characterization of starch-based films

Microalgal biomass processing was repeated for higher amount of biomass to have sufficient starch for the synthesis. 26 g of dry biomass with 31 % starch content were treated for lipid extraction with ethanol as previously described (see supplementary material) to obtain the defatted biomass sample (DMS). DMS (50 % starch content) was then treated with sonication in DMSO, followed by ethanol precipitation, as

previously described, apart from little variations of the sonication conditions: 1.6 g defatted biomass in 100 mL DMSO, 160 min at 60 % amplitude and t_{on} = 0.2 s, t_{off} = 0.2 s. The sample collected from precipitation was the purified microalgal starch sample (PMS).

Microalgal starch sample (MS) was blended with chitosan (CHIT, molecular weight 190–310 kDa, viscosity 200–800 cps, 75–85 % deacetylation degree) to prepare films (2D-matrices) by solvent casting. The process started by suspending 3 % (w/v) MS sample in 12.5 mL distilled water at 90 °C under stirring (800 rpm) for 90 min, for the gelatinization process. Then, 12.5 mL of a CHIT solution (2 % w/v) in 1 % w/v acetic acid was added and mixed for 20 min. Finally, temperature was decreased to 40 °C and glycerol was added at 10 % w/w of MS mass, as plasticizer, and mixed for 20 min. The final solution was then poured into a Teflon Petri dish with 6 cm diameter and dried at room temperature for 4 days. Three different chitosan/starch blends using different starch samples were made: with corn starch (CS), used for comparison; with DMS and with PMS.

The obtained film had the following composition with respect to the dry weight: 56.6 % starch sample (CS, DMS or PMS), 37.7 % chitosan and 5.7 % glycerol.

The films were called CS-CHIT, DMS-CHIT and PMS-CHIT and characterized as described in detail in a previous study (Tedeschi et al., 2021). Thermogravimetric analysis (TGA) was performed by Mettler TG 50 thermobalance on 6–8 mg of sample in a thermal range from 25 to 500 °C, under N_2 flow and at a heating rate of 10 °C min^{-1}. Mechanical properties: Tensile Strength (TS), Young's Modulus (E), Elongation at break (ε) and Toughness (T) of the prepared films were measured using an INSTRON 4502 (Instron Inc., Norwood, MA, USA). Films were cut into rectangular specimens (5 cm × 0.5 cm × 0.2 mm) and measurements were carried out at 10 mm min^{-1} deformation rate, using a 2 kN load cell. Water vapor permeability test was performed by the ASTM method E96 (Standard Test Methods for Water Vapor Transmission of Materials) with some modifications: circle shape films were fixed on the glass containers entrance (d = 8.4 cm and h = 4.5 cm) containing 3 mL of water. The vial weight was monitored during time (from 0 to 5 h) and water vapor transmission rate (WVTR) was calculated in triplicate at 5 h. The swelling ability of polymer films was obtained by immersing weighted films in water. At predetermined times (from 0 to 120 min), films were collected and weighted after removal of extra solvent with filter paper. The soluble fraction was measured by submerging a weighted sample for 2 h in water and then drying it for 24 h at room temperature. Light absorbance of the films was measured at 580 nm in a single-beam UV–Vis Spectrophotometer, HP DIODE ARRAY, (HP8452A, Hewlett Packard, Palo Alto, CA, USA) on a 5 x 30 mm specimen, and used to calculate the opacity as A_{580}/h, with h equal to the film thickness (mm).

2.9. Statistical treatment of data

All experiments were carried out in duplicate except for WVTR, made in triplicate. All data are reported as mean ± standard deviation (SD). The significance of the difference between sample means has been assessed by statistical tests: *t*-test and analysis of variance (ANOVA) followed by Tukey's HSD (honestly significant difference) test. The tests were performed using Microsoft Excel and R. For calculations including experimental data, the resulting error was calculated using the equations for error propagation. Difference have been considered statistically significant when $p < 0.05$.

3. Results and discussion

The biorefinery conceptual scheme investigated in this work includes a first phase in which lipids are the first compounds extracted (Fig. 1). Various reasons motivate this choice: lipids include molecules with high added value (fatty acids, carotenoids) that can be the most valuable product of the biorefinery; therefore, extracting them initially can allow for a higher recovery of the product with more added value (Ansari et al., 2017). Additionally, lipids consist of many sensitive molecules

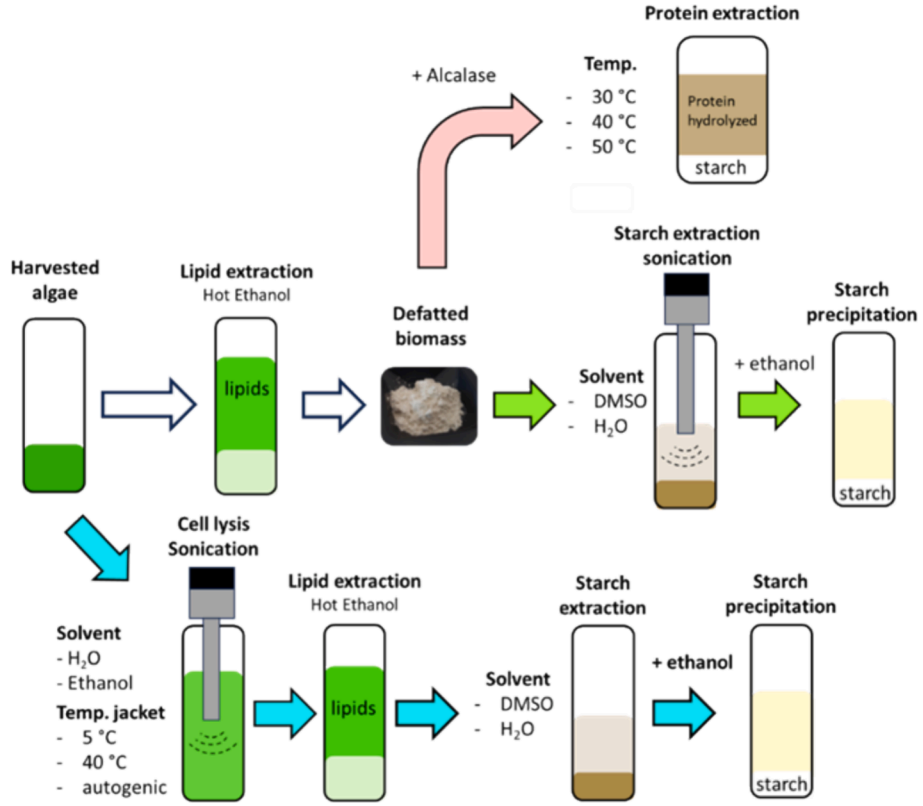

Fig. 1. Schematic representation of the different biorefinery routes tested for starch refinery from microalgae.

that are easily degradable during storage and chemical and physical treatments. Following the extraction of lipids, the resulted biomass obtained is primarily composed of starch, proteins, and cell-wall components (e.g. cellulose, sporopollenin) (Alhattab et al., 2019). The main challenge addressed by this study is to develop a process to separate starch from such other compounds.

3.1. Treatment with Alcalase (subtilisin A)

The use of enzymatic treatment for protein hydrolysis was driven by the idea that selectively extracting proteins would allow for the recovery of high-purity starch in the residual pellet, with also extracting a high-value protein hydrolysate. Various previous studies have investigated protein extraction from raw and defatted microalgae using various methods, including enzymatic treatment with protease (Gerde et al., 2013; Sari et al., 2013). However, these studies did not pay attention to the recovery of starch in the residual pellet. Alcalase has an optimal catalytic activity at around 60 °C (Ramalho and de Castro, 2023). However, this study was conducted between 30 and 50 °C due to the gelatinization temperature of starch of this microalgae, which was found to be between 45–55 °C (Di Caprio et al., 2022). To prevent starch gelatinization in the aqueous phase, temperatures over 50 °C were avoided. Across all tested temperatures, good protein extraction efficiencies were achieved after 2 h, ranging from 70 ± 3 % at 30 °C to 90 ± 10 % at 50 °C (Fig. 2a). At 40 °C and 50 °C, no significant increase in protein extraction efficiency was detected with longer treatment times, while at 30 °C extraction efficiency slowly increased to 83 ± 1 % after 5 h ($p = 0.03$). The protein extraction efficiency achieved in this study is higher than those reported in previous studies on microalgae using proteases (Rojo et al., 2021; Sari et al., 2013). The use of defatted biomass may explain this improved result (Sari et al., 2013). Negative control groups without enzyme exhibited negligible protein extraction efficiency, ranging between 2.5–10 %, with no effect of extraction time, likely due to the limited content of water-soluble proteins. Starch recovery (Y_{starch}) gradually decreased as the temperature increased, from 75 ± 7 % at 30 °C to 28 ± 2 % at 50 °C ($p = 0.01$). The most relevant decrease occurred between 40–50 °C, attributable to starch gelatinization (Fig. 2b). When tests were conducted without enzymes, there was no significant decrease in Y_{starch}, which remained constant at 84 ± 6 %. This result suggests that cell wall rupture operated by proteases is crucial for the extracellular release of starch. Biomass recovery followed a similar trend to starch recovery (Fig. 2b). Starch content inside biomass increased slightly after lipid extraction, from 38 ± 5 % to 45 ± 2 % ($p = 0.17$), due to the selective extraction of lipids by ethanol

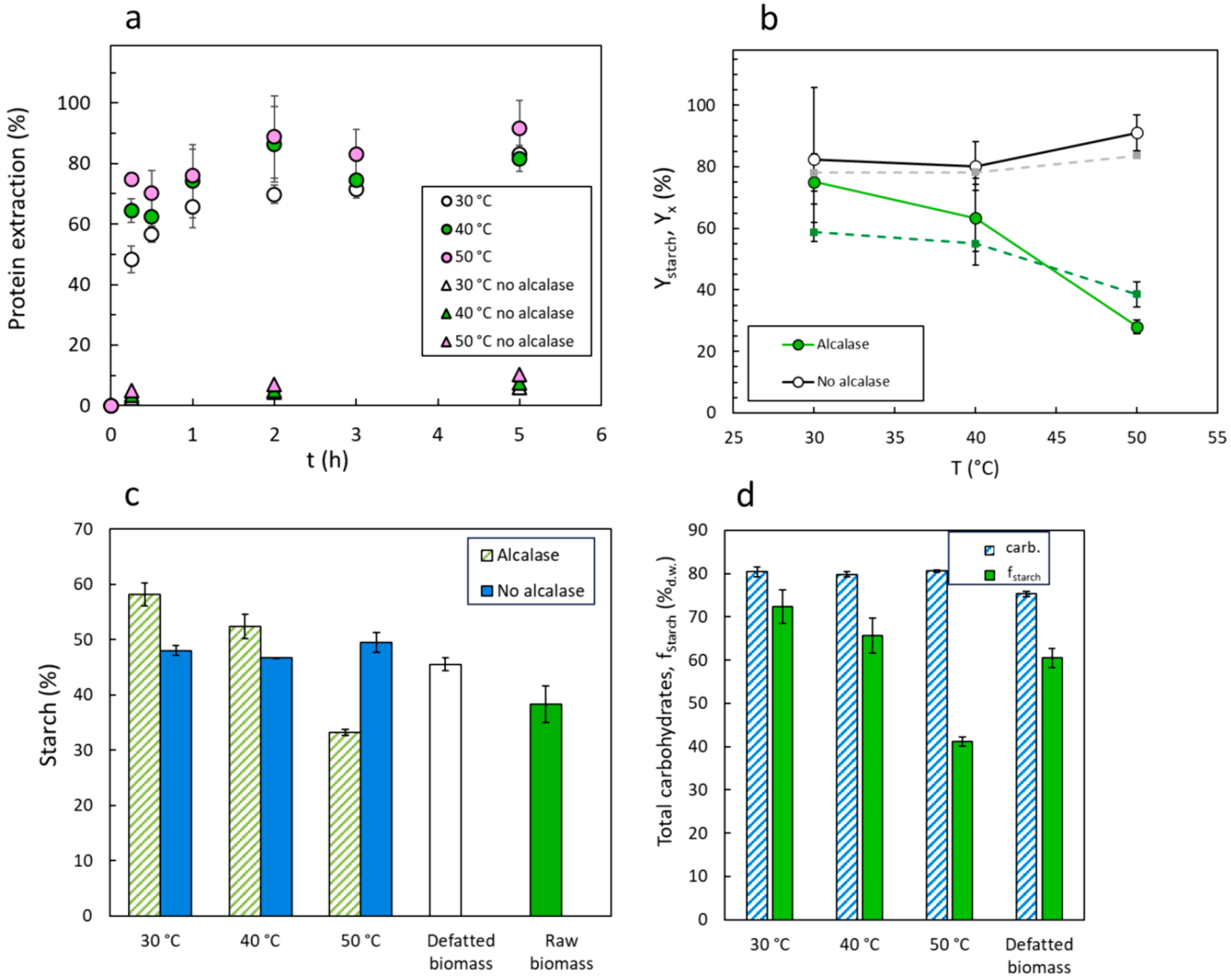

Fig. 2. Results for protein extraction on defatted biomass with Alcalase. A) Kinetics of protein extraction efficiency for different reaction temperatures, along with the control tests without Alcalase. B) Continuous lines indicate the final starch recovery (Y_{starch}), while dashed lines indicate the final biomass recovery (Y_X), both in the residual pellet. C) Starch content in the different samples before and after treatment. D) Total carbohydrate content and fraction of starch relative to total carbohydrates for the different samples before and after treatment.

(Fig. 2c). After lipid extraction, the starch content could be significantly increased by using enzymatic treatment (Fig. 2c), up to a maximum value of 58 ± 3 % with treatment at 30 °C (p = 0.03). However, temperature has a significant effect on the starch content in the recovered pellet (p = 0.004). As temperature increased, the starch content in the pellet decreased, reaching a minimum value of 33.2 ± 0.8 % at 50 °C. In the controls without enzyme, there was no significant variation in starch content regardless of the temperature used (p = 0.23). In terms of total carbohydrates, the recovery showed a trend comparable to starch, with values of 63 ± 5 %, 58 ± 9 % and 41 ± 3 % at 30 °C, 40 °C and 50 °C respectively. Total carbohydrate content increased significantly after enzymatic treatment compared to defatted biomass, rising from 75.3 ± 0.8 % to an average value of 80.3 ± 0.9 % (p = 0.02). This increase remained consistent regardless of the temperature used for the enzymatic treatment (Fig. 2c). The fraction of starch/total carbohydrates did not remain constant; it slightly increased after enzymatic treatment at 30 °C, from 0.61 ± 0.02 g g^{-1} to 0.72 ± 0.03 g g^{-1} (p = 0.04), while it decreased to 0.41 ± 0.01 g g^{-1} (p = 0.004) when the treatment was performed at 50 °C. This behavior confirms a gelatinization-induced loss of starch in water when enzymatic treatment was performed at 50 °C, while other carbohydrates (likely cell-wall cellulose)(do Carmo Cesário et al., 2022) didn't dissolve proportionally.

Among the various conditions tested for enzymatic treatment, the condition at 30 °C for 5 h was the most effective for recovering a pellet phase enriched in starch. The maximum starch content achieved in the residual pellet was 58 %, comparable to a previous study in which starch refining was conducted using cell disruption followed by ethanol extraction (Di Caprio et al., 2023). This starch content demonstrated suitability for producing plastic films with mechanical properties comparable to films made with pure corn starch (Di Caprio et al., 2023). One advantage of the enzymatic process is its effectiveness without the need for energy-intensive physical cell disruption methods (e.g. sonication). Additionally, the resulting protein hydrolysate extract has a potential applicability in bio-stimulants and other high-value products (Colla et al., 2017).

3.2. Starch extraction with solvent from defatted biomass

An alternative method for separating starch from other cellular components could involve selective starch extraction from defatted biomass, followed by its precipitation with ethanol. To test this strategy, defatted biomass containing 45 % starch was treated with boiling water and hot DMSO (80–100 °C), both solvents known for their ability to dissolve starch (Schmitz et al., 2009). Since pure DMSO and water are also known to be ineffective at solubilizing cellulose and other macromolecules (Ren et al., 2021; Seymour and Johnson, 1976), these solvents could potentially enable starch refinement. Ethanol was added to the resulting starch-containing supernatant in a 3:1 vol ratio to precipitate starch. When defatted biomass was subjected to extraction with hot DMSO, starch extraction was negligible (<10 %) at both 80 and 100 °C (Fig. 3a). However, the use of sonication remarkably enhanced starch extraction in DMSO, achieving up to 82 ± 7 % (p = 0.005), and yielding starch with increased purity of up to 81 ± 6 % after precipitation. Sonication facilitated starch release by disrupting cell walls and raising the temperature of the DMSO. Pulsed sonication was crucial in preventing excessive heating of the DMSO. In this experiment a t_{off}/t_{on} = 0.1/0.4 s was used, but it might change depending on the specific experimental setup. This protocol kept DMSO temperature between 80–100 °C for most of the treatment (Fig. 3b). This temperature range is considered optimal for starch extraction in DMSO, as it is high enough to allow solubilization but low enough to prevent its degradation (Schmitz et al., 2009). DMSO is a solvent with low toxicity, potentially suitable for food and pharmaceutical applications. However, using water as a solvent for starch extraction could be more cost-effective for industrial applications. Boiling water without sonication extracted 44 ± 3 % the starch, approximately 7 times more than DMSO without sonication. The

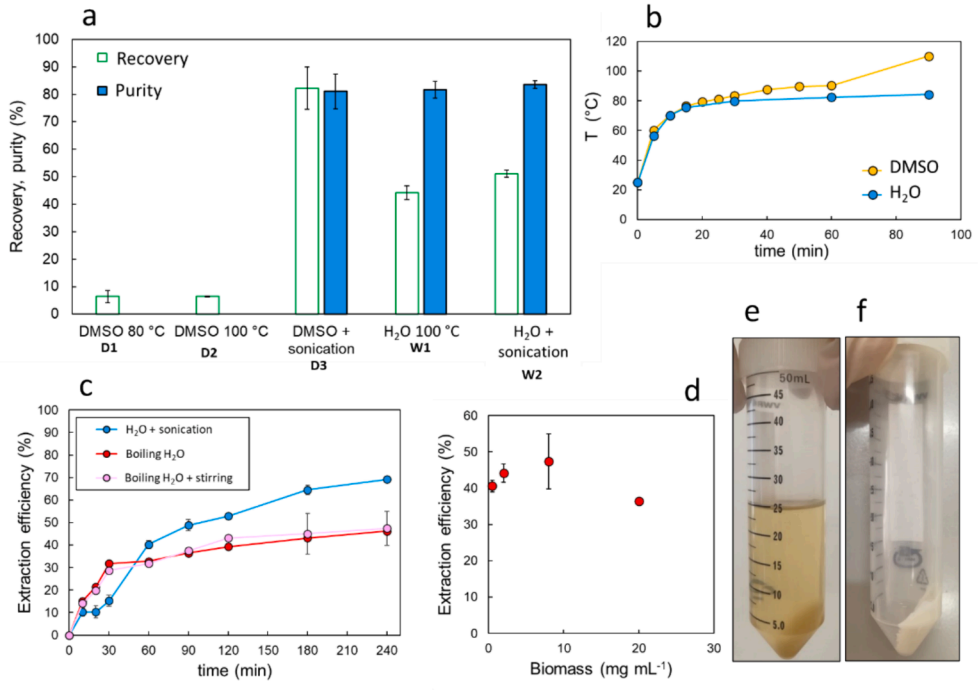

Fig. 3. Results from tests on starch extraction from defatted biomass with hot DMSO and water. A) Final recovery (%) and purity of starch extracted with 90 min treatment, after precipitation with ethanol. B) Variation in temperature during starch extraction in DMSO (D3) and water (W2) under ultrasonication treatment. C) Effect of the application of sonication (t_{on}/t_{off} = 0.1/0.2) and mechanical stirring during extraction in hot water. D) Effect of different defatted biomass concentration on the starch extraction efficiency in boiling water after 240 min of treatment. E) Sample after extraction in DMSO under sonication. F) Final purified starch precipitated with ethanol.

purity of the recovered starch after precipitation was similar to that obtained with DMSO (Fig. 3a). Sonication in water was less effective than in DMSO, showing only a negligible increase in starch extraction ($p = 0.076$) (Fig. 3a). This may be because water's operating temperature is closer to its boiling point, leading to excessive bubbling, which reduces sonication efficiency. When sonication is performed near the boiling point, the applied power decreases remarkably, possibly due to reduced solvent density caused by overbubbling (Di Caprio et al., 2023, 2021a). Various attempts were made to enhance starch extraction in water, assessing the effects of extraction time and mechanical stirring (Fig. 2c). In boiling water, with or without mechanical stirring, no significant increase in starch extraction was observed for times longer than 90 min. However, with sonication, a further increment was observed after 90 min, from 49 ± 2 % to 69 ± 2 % at 240 min of treatment (corresponding to $T_{on} = 80$ min). This latter value is comparable to that achieved with DMSO ($p = 0.14$). Lastly, the possibility to use different biomass to solvent ratio was tested; however, reducing biomass concentration to 0.5 mg mL^{-1} or increasing it to 20 mg mL^{-1} did not affect extraction efficiency ($p = 0.19$) (Fig. 3d), indicating no limitation due to the achievement of a saturation concentration. These experiments indicate that cell disruption is necessary to extract starch from defatted biomass using hot water or DMSO. Sonication is more effective in DMSO, but comparable efficiencies can be achieved with water by extending the treatment time.

3.3. *Exploring the configuration with cell lysis applied before lipid extraction*

The initial experiments reported in this work show that starch can be extracted at high percentages using either boiling water or DMSO. However, cell disruption remains a crucial requirement for the release of starch into the solvent. In biorefinery processes, cell disruption is typically carried out after harvesting to enhance the subsequent cascade extractions (Mittal and Ranade, 2023). Moreover, implementing a dedicated cell disruption step allows for direct operation under optimal conditions for cell lysis. A recent study indicates that the temperature employed during the sonication of microalgae can significantly affect the efficiency of this treatment (Di Caprio et al., 2023). Therefore, in this study, two solvents were systematically investigated (water and ethanol) at three different temperatures: *i*) without temperature control (autogenous temperature), *ii*) with cooling water at 5 °C, and *iii*) with cooling water at 40 °C.

Ethanol was tested with the aim of coupling cell lysis with lipid extraction and minimizing starch loss.

The condition (*i*) allowed the system to reach a temperature close to the solvent's boiling point; cooling water at 5 °C aimed to maintain a temperature near ambient temperature, while the condition (*iii*) aimed at investigating an intermediate temperature. In both ethanol and water, variations in operating temperature affected the kinetics of cell lysis and the maximum lysis achieved at the end of the treatment (Fig. 4a and b). The temperature inside the reactor was consistently higher than inside the jacket, due to heating induced by sonication. Almost all conditions attained a stable temperature after 5 min (Fig. 4c and d). Only in ethanol

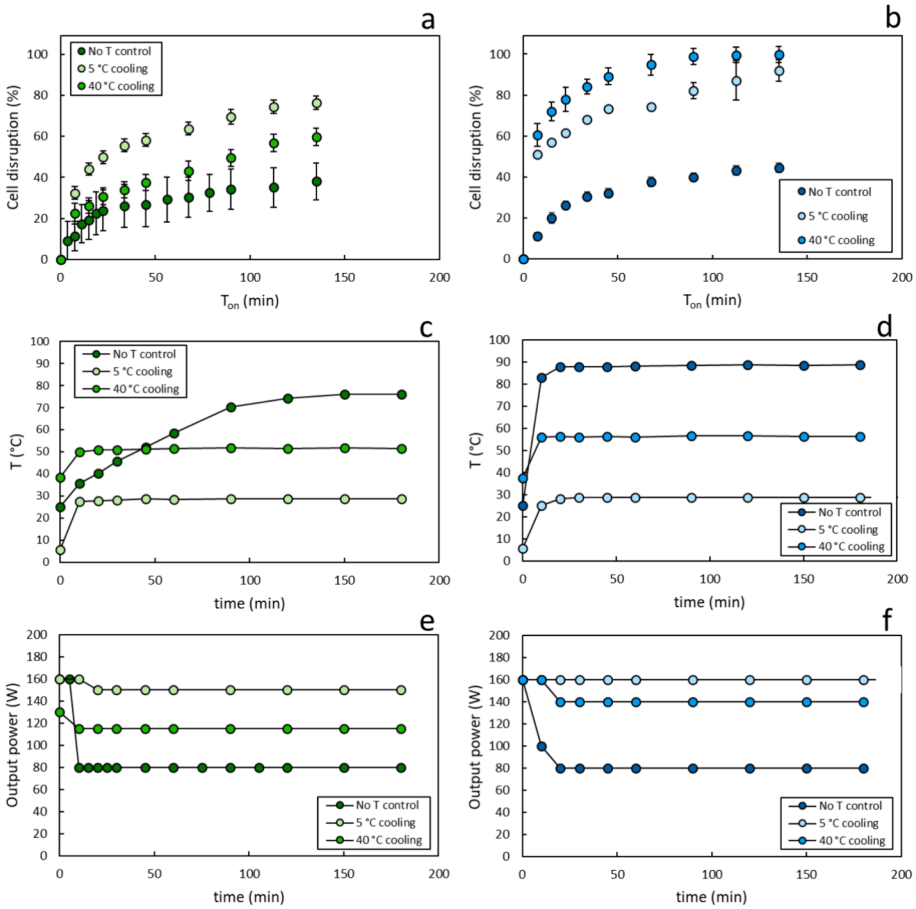

Fig. 4. Kinetics of cell disruption of microalgae with sonication, at different operative temperatures, using ethanol (left) and water (right) as solvent. In a) and b) the cell disruption efficiency measured at different treatment times are reported. In c) and d) the temperature measured inside the reactor are reported. In e) and f) the output powers applied by the ultrasonic probe to maintain the set amplitude are reported.

without temperature control, the increase in temperature was slower, taking about 90 min to stabilize. The operating temperatures achieved approximately 50 °C in the intermediate condition and 25–30 °C in the lower condition, for both ethanol and water. Without temperature control, the temperatures approached the respective boiling points of the solvents.

In the case of ethanol, the highest disruption rate was observed at the lower temperature, consistent with previous reports (Di Caprio et al., 2023). In contrast, with water, the highest disruption rate was achieved at the intermediate condition (~ 55 °C), with increase between 7–20 % compared to the treatment at 25–30 °C ($p = 3 \bullet 10^{-11}$) and up to 47 % compared to the treatment without temperature control (Fig. 4b). However, the difference with respect to the intermediate condition became negligible at the end of the treatment ($p = 0.25$). For both solvents, the least efficient cell disruption was observed without temperature control. This effect may be due to bubbling near the boiling point, which reduced the apparent density of the solvent and led to decreased applied power, as shown in the Fig. 4e and f. Indeed, the applied power in treatment without temperature control was half that observed at the lower temperature. The superior cell lysis observed in water at controlled temperature (25–30 °C) aligns with previous findings (Di Caprio et al., 2023). Furthermore, this study's results demonstrate that better lysis is achieved with water at the intermediate temperature (~ 55 °C) ($p = 0.01$), while no significant difference was found between the solvents when sonication was performed without external temperature control ($p = 0.43$). Analysis of the residual pellet recovered after

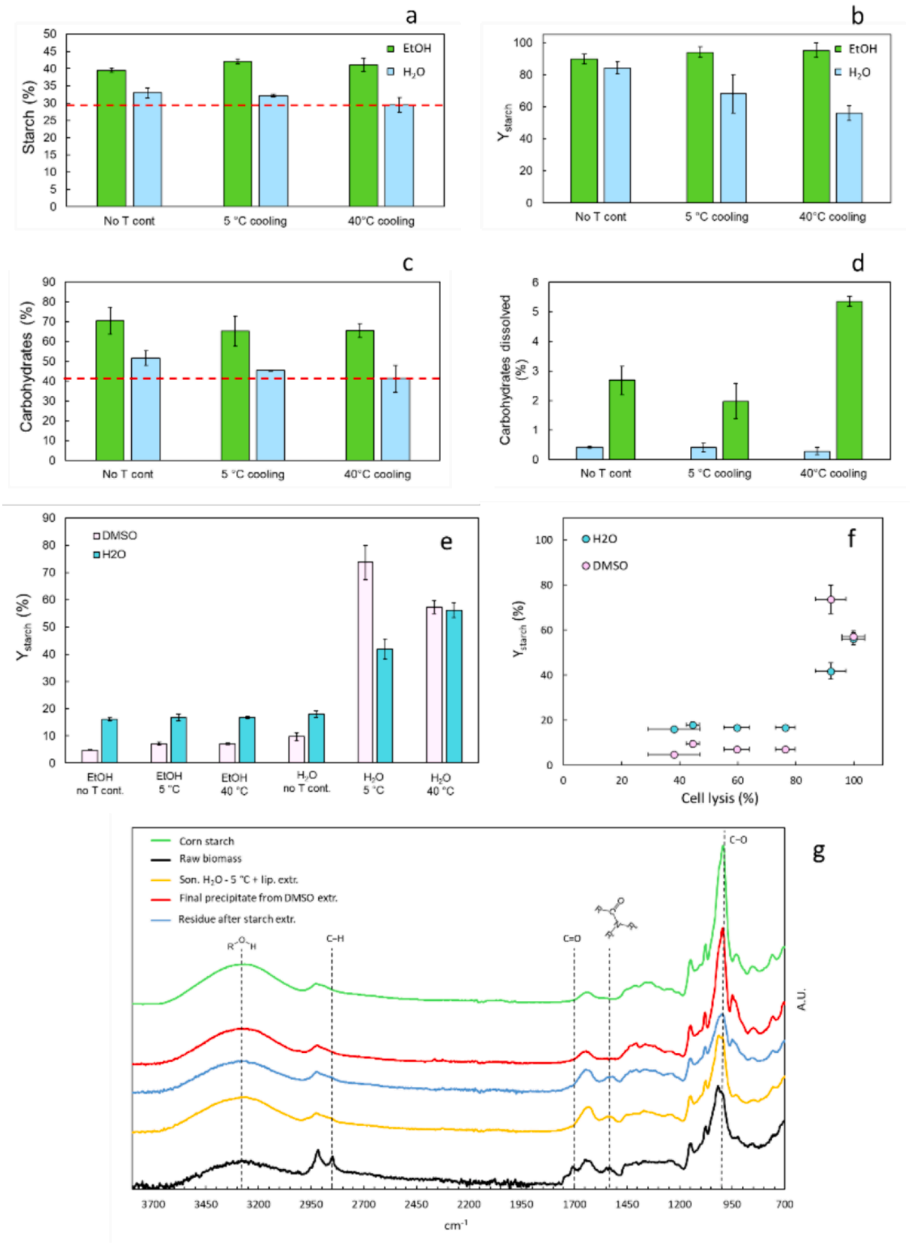

Fig. 5. A) Content of starch in the residual pellet recovered after cell lysis with sonication performed in different conditions. B) Starch recovery in the residual pellet after sonication. C) Total carbohydrate content in the residual pellet after sonication. D) Residual content of carbohydrates (as percentage with respect to the biomass) in the liquid phase (supernatant) after sonication. The dashed lines indicate the values in the raw biomass before sonication. E) Final starch recovery at the end of the whole extraction process: sonication of fresh biomass in different conditions (with ethanol or H_2O, at three different temperatures as indicate in the X-label), then followed by lipid extraction with ethanol, starch extraction in DMSO or water at 100 °C, and finally precipitation with ethanol. F) Relation between final cell lysis obtained with the different sonication conditions tested and final starch recovery after precipitation with ethanol. G) ATR-FTIR spectra of the pellets obtained with the different treatments compared with raw biomass and pure corn starch.

sonication indicated that, when sonication was performed in water, there was no significant variation in starch content (Fig. 5a) ($p = 0.13$). When sonication was performed in ethanol, the starch content increased from the initial 29 ± 2 % of the raw biomass to an average of 41 ± 2 % ($p = 0.0005$), regardless of the temperature during sonication. This increase was likely due to lipid extraction in ethanol. FTIR analysis confirmed this explanation, as all the pellets obtained after sonication in ethanol showed a remarkable reduction of the characteristic fatty acid peaks of $–CH_2$ and —C═O at 3000–2800 cm^{-1} and 1750–1680 cm^{-1} respectively (see supplementary material). The same trend was observed for total carbohydrates (Fig. 5c), which increased from 40 ± 5 % to an average of 67 ± 3 % after sonication in ethanol ($p = 0.001$). Starch recovery after sonication in ethanol was, on average, 93 ± 3 %, irrespective of the temperature employed (Fig. 2b). When sonication was performed in water, the recovery decreased to an average of 70 ± 10 %, significantly lower than with ethanol ($p = 0.018$). In the residual supernatants after sonication, only a negligible amount of carbohydrates remained, between 0.3–5.3 % of the initial amount (Fig. 5d).

3.4. Extraction of starch in DMSO or water after cell lysis and lipid extraction

Each sample pre-treated with sonication for cell lysis, at the different conditions described in the previous section, was further processed for lipid extraction, followed by starch extraction. Lipid extraction was conducted using the same protocol for all samples, based on ethanol extraction. After lipid extraction, the starch content significantly increased ($p = 1 \bullet 10^{-5}$), with 3.1–7.5 % improvements (see supplementary material). Following lipid extraction, the starch content varied between 35–47 %, while total carbohydrates ranged between 58–73 % (see supplementary material). Starch extraction was then tested using both DMSO and water at 100 °C, without sonication during the extraction process. Only two pre-treatments allowed to attain a Y_{starch} comparable to the previous tests (Fig. 5e), where sonication was applied during starch extraction. These pretreatments were those where sonication was performed in water at 5 °C or 40 °C, which also correspond to the conditions where the highest cell disruptions were achieved. There is a relationship between Y_{starch} in water and DMSO and the preceding cell lysis efficiency (Fig. 5f). For cell lysis < 80 %, Y_{starch} remained constant at 7 ± 2 % in water and 16.9 ± 0.8 % in DMSO. For these samples, water allowed higher Y_{starch} ($p = 10^{-8}$), possibly because of a certain positive contribution by hot water on cell lysis. For cell lysis > 80 %, the best result, $Y_{starch} = 74 \pm 6$ %, was achieved with DMSO on sample sonicated in water with cooling water at 5 °C. DMSO confirmed to be a more effective solvent than water ($p = 0.025$). The starch obtained from this treatment was precipitated with ethanol, yielding a precipitate with 91.2 ± 0.4 % purity. This is a notable high purity for microalgal starch obtained through a refinery process that does not include centrifugation through a Percoll gradient. The residual pellet remaining after DMSO extraction was analyzed and showed a residual starch content of 4.6 ± 0.2 %, confirming the effectiveness of the extraction.

To have an independent assessment of the starch purity, FTIR analysis was carried out on the samples obtained after the different treatments (Fig. 5g). In the 3000–2800 cm^{-1} range, characteristic bands of $–CH_2$ and $–CH_3$ groups, present in lipids, were identified, while the —C═O groups of fatty acids were identifiable by a peak at 1750–1680 cm^{-1} (Laurens and Wolfrum, 2011). Proteins were identified by amide I and amide II adsorption bands of the peptide bond between 1700–1450 cm^{-1} (Arrondo and Goñi, 1999). Raw biomass showed a larger number of peaks, due to the presence of relevant amounts of lipids, starch, proteins and other compounds. After sonication and lipid extraction, a remarkable reduction in the peaks of lipids was observed, while peaks of peptide bonds remain well visible between 1700–1450 cm^{-1}. The final starch sample obtained after DMSO extraction and precipitation with ethanol showed the disappearance of the peak at 1538 cm^{-1} (amide II), indicating the complete removal of proteins. The spectrum of the final microalgal starch was identical to that of pure corn starch (Fig. 5g), confirming the high purity of the sample. In contrast, the residual pellet remained undissolved after DMSO extraction showed a remarkable presence of protein peaks, confirming that proteins remained in the pellet.

3.5. Comparison among the different biorefinery routes

In this study, starch extraction recovery was calculated for each unit operation within the investigated biorefinery routes. These data enabled the calculation of overall starch recovery in the various process configurations (Table 1). Through enzymatic treatment, a final starch purity of 58 % with a recovery of 70 % was achieved. This purity can be adequate for the synthesis of plastic films (Di Caprio et al., 2023). Additionally, this biorefinery route allows for the efficient extraction of both lipids and proteins. These can be utilized in high-value applications as bioactive compounds, such as for the production of nutraceuticals and agricultural bio-stimulants (Munaro et al., 2024). An additional advantage of this process is avoiding sonication, which can pose challenges during the scale-up, due to its associated energy consumption (Di Caprio et al., 2022). However, the cost of pure enzymes used must be carefully assessed, considering the final markets of the resulting products. When sonication was directly applied during DMSO extraction on defatted biomass, the highest starch recovery (80 %) was achieved. Sonication with DMSO on defatted biomass also resulted in a starch purity of 81 %, significantly higher than that obtained with enzymatic treatment ($p = 0.04$). In the process where cell lysis was conducted before lipid extraction, the highest starch purity (91 %) was achieved, though with a reduced starch recovery of 63 %. This lower recovery can be attributed partly due to the application of 4-unit operations instead of 3, and partly to the lower recovery obtained from DMSO extraction. The differences in recovery among the compared processes were not statistically significant. It's important to note that the lack of significant difference among the overall recoveries was likely influenced by relatively high associated errors. Errors in final recovery were calculated using error propagation formulas, which inevitably resulted in increased uncertainty.

There is no single process configuration that is universally better than the others. Case-by-case assessments should be conducted, depending on the final application, as each has specific constrains regarding cost and product quality targets. In this study, the objective was to produce starch-based plastic films. For this application, the process in which DMSO extraction was carried out during sonication was chosen, as it offered the best compromise between extraction recovery, purity, and workload.

Table 1
Comparison between the three different biorefinery routes studied in this work for extracting and purifying starch from microalgae biomass.

Enzymatic treatment				
Lipid extraction Y_{starch}	Protein extraction Y_{starch}	Final Y_{starch}		Purity
0.97 ± 0.11	0.75 ± 0.07	0.7 ± 0.1		58 ± 3 %
Direct sonication of defatted biomass in DMSO				
Lipid extraction Y_{starch}	DMSO extraction + precipitation Y_{starch}	Final Y_{starch}		Purity
0.97 ± 0.11	0.82 ± 0.08	0.8 ± 0.1		81 ± 6 %
Sonication → Lipid Extraction → DMSO extraction				
Cell lysis Y_{starch}	Lipid extraction Y_{starch}	DMSO extraction + precipitation Y_{starch}	Final Y_{starch}	Purity
0.94 ± 0.03	0.91 ± 0.04	0.74 ± 0.06	0.63 ± 0.06	91 ± 4 %

3.6. Production of plastic film using microalgal starch

Due to its low cost and renewability, starch is considered a valid material to produce biodegradable films for packaging applications in replacement of fossil-based polymers. However, the application of starch in this sector is limited by its brittleness and low water resistance (Chaléat et al., 2014). To overcome these drawbacks, starch is usually plasticized with polyols (e.g., glycerol) (Ma et al., 2023) or used as a component in composites and blends (Jayarathna et al., 2022). The applicability of microalgal starch was assessed in this study by comparing the properties of films produced using corn starch (as control), with the use of defatted microalgal biomass (50 ± 1 % starch) and purified microalgal starch (81 ± 6 % starch) produced from DMSO extraction under sonication from defatted biomass, followed by precipitation with ethanol.

The production of a plastic film with microalgal starch was described so far only in a prior study (Di Caprio et al., 2023). In this work the authors obtained a sample with 56 % starch, which is comparable to the sample of defatted biomass (DMS). In this previous work the synthesis of the film was carried out mixing starch with only water and 30 % glycerol, as plasticizer, obtaining a film comparable to that one obtained with corn starch, but with limited mechanical properties. The aim of this work was to improve physical and mechanical properties of films made with microalgal starch. To this aim the amount of glycerol was lowered

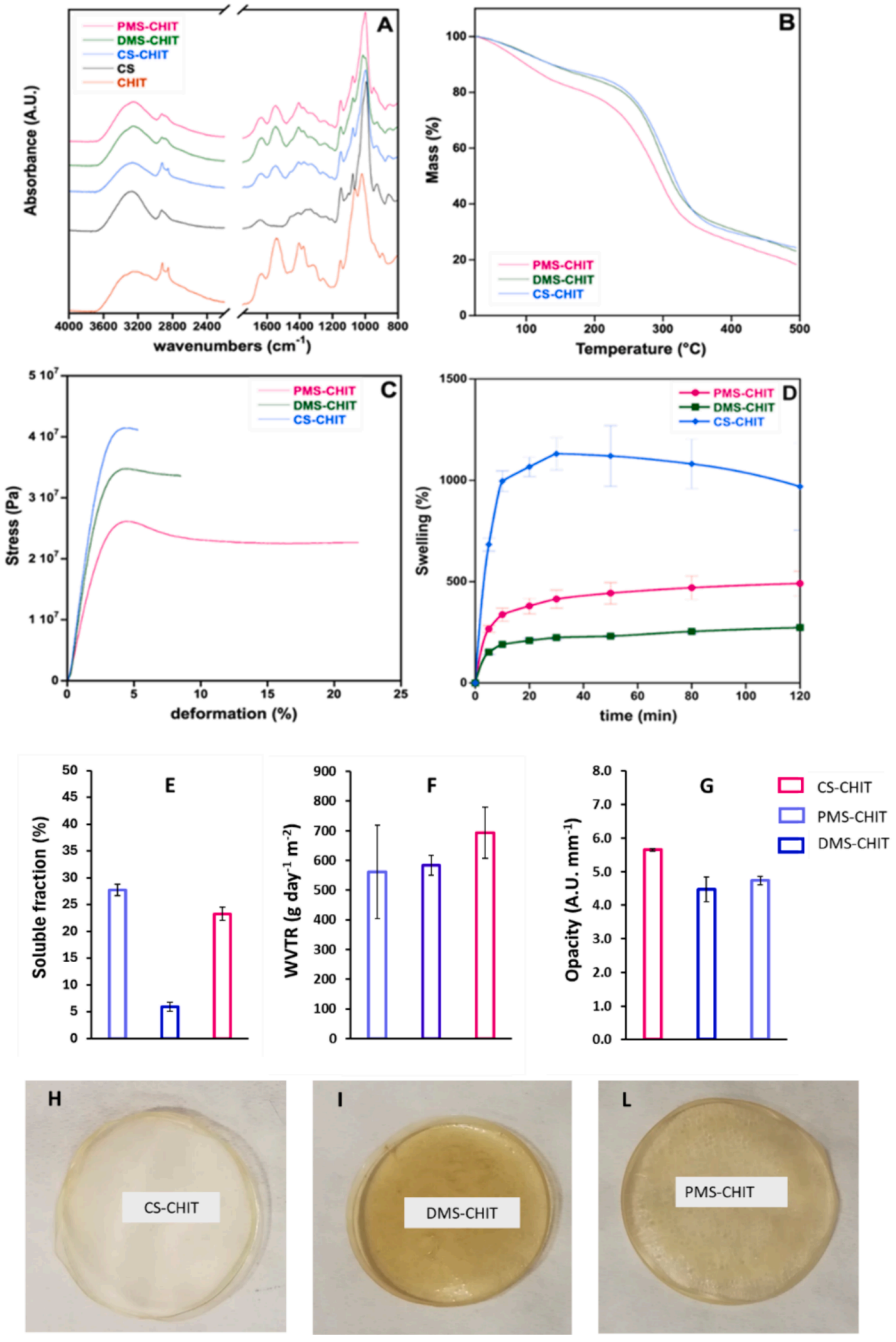

Fig. 6. Results from plastic film preparation. ATR-FTIR spectra (A), thermogravimetric curves (B), stress–strain curves (C) and swelling in water (D) of CHIT and of the produced CS-CHIT, DMS-CHITS, and PMS-CHIT films. Comparison among plastic films obtained with chitosan-corn starch (CS-CHIT), chitosan-defatted microalgae (DMS-CHIT) and chitosan-purified microalgal starch (PMS-CHIT) for soluble fraction (E), WVTR (F) and transmittance (G). Data are reported as mean ± SD (n = 2). In H, I and L, pictures of the obtained films are shown.

to 10 % and chitosan was blended to produce plastic films. Indeed, previous studies demonstrated the ability of chitosan in improving the tensile strength of starch based films (Jantanasakulwong et al., 2016), as well as on providing antimicrobial properties (Perdana et al., 2021).

In Fig. 6A, the FTIR spectra of the pristine materials, corn starch (CS) and chitosan (CHIT), and the blended samples CS-CHIT, DMS-CHIT and PMS-CHIT are reported. All spectra showed a broad band from 3700 to 3000 cm^{-1}, attributed to the stretching vibrations of free O—H groups (Dai et al., 2019), whereas peaks in the range 3000–2800 cm^{-1} are associated to the C—H stretching (–CH_2, 2920 cm^{-1}; –CH_3, 2855 cm^{-1}). In CHIT spectrum, O-H vibrations overlapped to the N—H bond stretching vibration (Bajer et al., 2020). Instead, stretching at 1650 cm^{-1} is attributed to the acetylate groups (amide I), as well as a peak at 1538 cm^{-1} is ascribed to the N—H bending of primary amines (amide II); bending vibrations at 1404 cm^{-1} and 1377 cm^{-1} are associated to methylene and methyl groups (Theophanides and Theophanides, 2012); a peak at 1311 cm^{-1} is related to the C—N stretching. The absorption peaks in the spectral range 1150–1020 cm^{-1} can be attributed to C—O—C and C—O—H stretching and the peak at 896 cm^{-1} to the C—O—C pyranose ring stretching (Brugnoli et al., 2023). In CS spectrum, the peak at 1640 cm^{-1} is related to the bending of the H—O—H bond of the absorbed water. Furthermore, absorption bands associated with C—O—H bending are present in the region of 1200 and 950 cm^{-1}, while the C—O—C stretching in the 950–700 cm^{-1} region (Romano et al., 2023).

When starch was blended with CHIT, an enlargement of the band related to O—H and N—H vibration was observed (Stuart, 2005), together with a shift from 1538 cm^{-1} to 1548 cm^{-1} in the absorption peak of the –NH_2 of chitosan, suggesting possible interactions between the hydroxyl groups of starch and the amino groups of CHIT, as previously reported (Bourtoom and Chinnan, 2008). No significant differences were found by comparing the spectra of the blends obtained with different types of starch, suggesting a similar behavior of microalgal and corn starch.

Thermal stability of the blended films was similar (Fig. 6B), with comparable degradation temperatures (T_d) ranging from 293 to 307 °C (Table 2). An initial weight loss (ca. 10 %) occurring around 100 °C can be attributed to absorbed water. The residual mass remaining at 500 °C is mainly due to CHIT, that forms cross-linked networks during thermal degradation (Zawadzki and Kaczmarek, 2010). A fraction of the residue is also made of ashes, and, for DMS-CHIT, of sporopollenin, as was described in a previous work (Di Caprio et al., 2023). PMS-CHIT showed a lower residue percentage (ca. 18 %), possibly because the purification step led to the removal of high-temperature resistance components as sporopollenin.

To study the mechanical performances of the starch-chitosan blends, tensile tests were performed. In Fig. 6C, the stress–strain curves of the blends are shown while the mechanical properties of the three films obtained are reported in Table 2. The Young's modulus (E) of the film made with corn starch (CS-CHIT) was two folds higher than with purified microalgal starch (PMS-CHIT) ($p = 0.02$), while comparable with defatted biomass (DMS-CHIT) ($p = 0.09$). Tensile strength (TS) was different among the three samples ($p < 0.01$), with the highest value for CS-CHIT, and the lowest value for PMS-CHIT (−45 % compared to CS-CHIT). Elongation at break (ε) and toughness (T) both showed an increasing trend towards more purified starch (Table 2), but the differences were not statistically significant, with p-value 0.07 and 0.052, respectively. When compared to the reference test where CHIT was not used, it is evident that CHIT increases about one order of magnitude the toughness and 2–5 fold the elongation at break, while the tensile strength was not affected by CHIT (Di Caprio et al., 2023). Blending with CHIT also reduces about 20–30 folds the elastic modules (Table 2). Such reduction is of minor magnitude when compared with films made with 30 % glycerol (Di Caprio et al., 2023). This finding suggests that CHIT may interfere with starch-starch interactions, by establishing hydrogen bonds with starch in replacement of the starch-starch inter and intramolecular H-bond interactions, weakening the structure and promoting deformation (Mendes et al., 2016). The blends obtained with different starch samples showed similar WVTR but different stability in water. The susceptibility or damage of materials in water environment is a key factor when a biodegradable material is used, as most biopolymers are hydrophilic (Jiménez-Regalado et al., 2021). To analyze the water stability of the obtained films, the swelling in water of each film was determined (Fig. 6D). Compared to corn starch (CS-CHIT), both samples with microalgal starch (DMS-CHIT and PMS-CHIT) showed up to 4 times lower swelling percentages ($p < 0.01$). Among them, DMS-CHIT appeared the most stable in water, with 5.9 ± 0.8 % soluble fraction, which is about 4–5 folds lower than for DMS-CHIT and PMS-CHIT ($p < 0.01$). Such a finding might be related to the higher content of insoluble impurities in the blend (cellulose, sporopollenin), which acted as strengthening fillers of the films. The film with corn starch was that one with the highest transmittance (12.5 ± 0.5 %), likely due to the thickness ≈10 % lower ($p = 0.0007$) and minor presence of impurities. Film thickness was 0.18 ± 0.01 mm for CS-CHIT, 0.198 ± 0.007 mm for PMS-CHIT and 0.204 ± 0.007 mm for DMS-CHIT. The opacity of the films was not statistically different among samples (slightly above 5 mm^{-1}), which is the maximum threshold for being considered a transparent material (Guzman-Puyol et al., 2022). The sample DMS-CHIT showed higher variability in the measured opacity, possibly due to higher heterogeneity caused by the presence of residual cell wall debris.

These results indicate that blending starch with chitosan was a successful strategy to improve material toughness (Table 2). The enhancement of toughness by CHIT is significant because it is a critical property for materials used in flexible packaging. Starch, while being a biodegradable and renewable resource, is inherently brittle, limiting its practical application in packaging solutions. By incorporating CHIT, blended films gain the needed toughness to withstand the stresses encountered during use. The biorefinery route applied has relevant impacts on the properties of the microalgal starch. Films with defatted microalgal showed better water stability and higher Young's modulus and tensile strength than purified microalgal starch, indicating higher rigidity. Instead, the results suggests that an increased purification of microalgal starch can improve toughness and elongation at break. Overall, although the differences in toughness among DMS and PMS starch types are not statistically significant, the trend highlights the potential benefits of using high-purity starch in combination with CHIT for creating more robust bioplastics. These insights could guide future research and development towards optimizing the composition of biodegradable packaging materials for enhanced performance. Further studies are required to elucidate the reasons of such differences. Likely, a relevant role is played by impurities, as sporopollenin, cellulose and proteins, that can improve the heterogeneity and act as points of weakness, but also as reinforcing fillers with lower water solubility. Possible modifications to starch during the sonication treatment might also have played a role (Airlangga et al., 2021).

Table 2
Properties of plastic films obtained with chitosan-corn starch (CS-CHIT), chitosan-defatted microalgae (DMS-CHIT) and chitosan-purified microalgal starch (PMS-CHIT). Young's modulus (E), Elongation at break (ε), Tensile strength (TS), Toughness (T). Data are reported as mean ± SD (n = 2). For each column, statistically significant differences among samples ($p < 0.05$) are indicated with different letters.

	E (MPa)	ε (%)	TS (MPa)	T (MPa)
CS	300 ± 100	3 ± 2^{a}	30 ± 1^{a}	0.34 ± 0.05^{a}
CS-CHIT	15.7 ± 0.1^{ab}	7 ± 2^{ab}	40.9 ± 0.2^{b}	2.8 ± 0.7^{b}
DMS-CHIT	12 ± 2^{a}	11 ± 3^{ab}	32 ± 2^{a}	2.5 ± 0.3^{b}
PMS-CHIT	8.5 ± 0.4^{b}	16.4 ± 0.6^{b}	22 ± 1^{c}	3.5 ± 0.1^{b}

4. Conclusions

A novel microalgae starch refining process was developed using extraction in hot water/DMSO followed by ethanol precipitation, achieving up to 91 % purity. Additionally, defatted microalgae treatment with Alcalase shows promise for integrating the production of starch with that of nutraceuticals/biostimulants.

Blending starch with chitosan shows positive effects on starch-based films, while the starch refining method significantly influences bioplastic properties, providing strategic approaches to tailor materials for specific applications. Future research should focus on evaluating the performances of the developed plastic materials for targeted applications.

CRediT authorship contribution statement

Fabrizio Di Caprio: Writing – review & editing, Writing – original draft, Visualization, Supervision, Resources, Methodology, Formal analysis, Conceptualization. **Nooshin Pedram:** Investigation, Data curation. **Benedetta Brugnoli:** Writing – original draft, Visualization, Formal analysis. **Iolanda Francolini:** Writing – review & editing, Supervision, Resources, Methodology, Conceptualization. **Pietro Altimari:** Writing – review & editing. **Francesca Pagnanelli:** Writing – review & editing, Supervision, Resources.

Declaration of competing interest

The authors declare that they have no known competing financial interests or personal relationships that could have appeared to influence the work reported in this paper.

Data availability

Data will be made available on request.

Acknowledgements

This work did not receive any specific funding. The authors wish to thank Maria Rita Caccavale and Giulia La Venuta for their contributions to experimental activities.

Appendix A. Supplementary data

Supplementary data to this article can be found online at https://doi.org/10.1016/j.biortech.2024.131516.

References

Airlangga, B., Sugianto, A.M., Parahita, G., Puspasari, F., Mayangsari, N.E., Trisanti, P. N., Sutikno, J.P., Sumarno, S., 2021. Study of cassava starch degradation using sonication process in aqueous sodium chloride. J. Sci. Food Agric. 101, 2406–2413. https://doi.org/10.1002/JSFA.10864.

Alhattab, M., Kermanshahi-pour, A., Brooks, M.S., 2019. Microalgae disruption techniques for product recovery : influence of cell wall composition. J. Appl. Phycol. 1, 61–88.

Ansari, F.A., Shriwastav, A., Gupta, S.K., Rawat, I., Bux, F., 2017. Exploration of Microalgae Biorefinery by Optimizing Sequential Extraction of Major Metabolites from Scenedesmus obliquus. Ind. Eng. Chem. Res. 56, 3407–3412. https://doi.org/10.1021/acs.iecr.6b04814.

Araújo, R., Vázquez Calderón, F., Sánchez López, J., Azevedo, I.C., Bruhn, A., Fluch, S., Garcia Tasende, M., Ghaderiardakani, F., Ilmjärv, T., Laurans, M., Mac Monagail, M., Mangini, S., Peteiro, C., Rebours, C., Stefansson, T., Ullmann, J., 2021. Current status of the algae production industry in europe: an emerging sector of the blue bioeconomy. Front. Mar. Sci. 7, 1–24. https://doi.org/10.3389/fmars.2020.626389.

Arrondo, J.L.R., Goñi, F.M., 1999. Structure and dynamics of membrane proteins as studied by infrared spectroscopy. Prog. Biophys. Mol. Biol. 72, 367–405. https://doi.org/10.1016/S0079-6107(99)00007-3.

Bajer, D., Janczak, K., Bajer, K., 2020. Novel starch/chitosan/aloe vera composites as promising biopackaging materials. J. Polym. Environ. 28, 1021–1039. https://doi.org/10.1007/S10924-020-01661-7/TABLES/6.

Bourtoom, T., Chinnan, M.S., 2008. Preparation and properties of rice starch–chitosan blend biodegradable film. LWT - Food Sci. Technol. 41, 1633–1641. https://doi.org/10.1016/J.LWT.2007.10.014.

Brugnoli, B., Mariano, A., Simonis, B., Bombelli, C., Sennato, S., Piozzi, A., Taresco, V., Chauhan, V.M., Howdle, S.M., Scotto d'Abusco, A., Francolini, I., 2023. Self-assembled chitosan-sodium usnate drug delivery nanosystems: synthesis, characterization, stability studies, in vitro cytotoxicity and in vivo biocompatibility against 143 B cells. Carbohydr. Polym. Technol. Appl. 6, 100373. https://doi.org/10.1016/J.CARPTA.2023.100373.

Chaléat, C., Halley, P.J., Truss, R.W., 2014. Mechanical Properties of Starch-Based Plastics. Starch Polym. From Genet. Eng. to Green Appl. 187–209. https://doi.org/10.1016/B978-0-444-53730-0.00023-3.

Colla, G., Hoagland, L., Ruzzi, M., Cardarelli, M., Bonini, P., Canaguier, R., Rouphael, Y., 2017. Biostimulant action of protein hydrolysates: unraveling their effects on plant physiology and microbiome. Front. Plant Sci. 8, 327435. https://doi.org/10.3389/FPLS.2017.02202/BIBTEX.

Dai, L., Zhang, J., Cheng, F., 2019. Effects of starches from different botanical sources and modification methods on physicochemical properties of starch-based edible films. Int. J. Biol. Macromol. 132, 897–905. https://doi.org/10.1016/J.IJBIOMAC.2019.03.197.

Di Caprio, F., Altimari, F., Pagnanelli, P., 2021a. Ultrasound-assisted Extraction of Carbohydrates from Microalgae. Chem. Eng. Trans. 86, 25–30. https://doi.org/10.3303/CET2186005.

Di Caprio, F., Tayou Nguemna, L., Stoller, M., Giona, M., Pagnanelli, F., 2021b. Microalgae cultivation by uncoupled nutrient supply in sequencing batch reactor (SBR) integrated with olive mill wastewater treatment. Chem. Eng. J. 410, 128417. https://doi.org/10.1016/j.cej.2021.128417.

Di Caprio, F., Chelucci, R., Francolini, I., Altimari, P., Pagnanelli, F., 2022. Extraction of microalgal starch and pigments by using different cell disruption methods and aqueous two-phase system. J. Chem. Technol. Biotechnol. 97, 67–78. https://doi.org/10.1002/jctb.6910.

Di Caprio, F., Amenta, S., Francolini, I., Altimari, P., Pagnanelli, F., 2023. Microalgae biorefinery: optimization of starch recovery for bioplastic production. ACS Sustain. Chem. Eng. 11, 16509–16520. https://doi.org/10.1021/ACSSUSCHEMENG.3C04133.

do Carmo Cesário, C., Soares, J., Cossolin, J.F.S., Almeida, A.V.M., Bermudez Sierra, J.J., de Oliveira Leite, M., Nunes, M.C., Serrão, J.E., Martins, M.A., dos Reis Coimbra, J. S., 2022. Biochemical and morphological characterization of freshwater microalga Tetradesmus obliquus (Chlorophyta: Chlorophyceae). Protoplasma 259, 937–948. https://doi.org/10.1007/S00709-021-01712-3/TABLES/1.

El Halal, S.L.M., Kringel, D.H., Zavareze, E. da R., Dias, A.R.G., 2019. Methods for Extracting Cereal Starches from Different Sources: A Review. Starch - Stärke 71, 1900128. https://doi.org/10.1002/STAR.201900128.

Fernández, F.G.A., Reis, A., Wijffels, R.H., Barbosa, M., Verdelho, V., Llamas, B., 2021. The role of microalgae in the bioeconomy. N. Biotechnol. 61, 99–107. https://doi.org/10.1016/j.nbt.2020.11.011.

Gerde, J.A., Wang, T., Yao, L., Jung, S., Johnson, L.A., Lamsal, B., 2013. Optimizing protein isolation from defatted and non-defatted Nannochloropsis microalgae biomass. Algal Res. 2, 145–153. https://doi.org/10.1016/j.algal.2013.02.001.

Gifuni, I., Olivieri, G., Krauss, I.R., D'errico, G., Pollio, A., Marzocchella, A., 2017. Microalgae as new sources of starch: isolation and characterization of microalgal starch granules. Chem. Eng. Trans. 57, 1423–1428. https://doi.org/10.3303/CET1757238.

Guzman-Puyol, S., Benítez, J.J., Heredia-Guerrero, J.A., 2022. Transparency of polymeric food packaging materials. Food Res. Int. 161, 111792. https://doi.org/10.1016/J.FOODRES.2022.111792.

Izumo, A., Fujiwara, S., Oyama, Y., Satoh, A., Fujita, N., Nakamura, Y., Tsuzuki, M., 2007. Physicochemical properties of starch in Chlorella change depending on the CO2 concentration during growth: comparison of structure and properties of pyrenoid and stroma starch. Plant Sci. 117, 1138–1147. https://doi.org/10.1016/j.plantsci.2007.03.001.

Jantanasakulwong, K., Leksawasdi, N., Seesuriyachan, P., Wongsuriyasak, S., Techapun, C., Ougizawa, T., 2016. Reactive blending of thermoplastic starch, epoxidized natural rubber and chitosan. Eur. Polym. J. 84, 292–299. https://doi.org/10.1016/J.EURPOLYMJ.2016.09.035.

Jayarathna, S., Andersson, M., Andersson, R., 2022. Recent Advances in Starch-Based Blends and Composites for Bioplastics Applications. Polym. 2022, Vol. 14, Page 4557 14, 4557. https://doi.org/10.3390/POLYM14214557.

Jiménez-Regalado, E.J., Caicedo, C., Fonseca-García, A., Rivera-Vallejo, C.C., Aguirre-Loredo, R.Y., 2021. Preparation and Physicochemical Properties of Modified Corn Starch–Chitosan Biodegradable Films. Polym. 2021, Vol. 13, Page 4431 13, 4431. https://doi.org/10.3390/POLYM13244431.

Laurens, L.M.L., Wolfrum, E.J., 2011. Feasibility of spectroscopic characterization of algal lipids: chemometric correlation of NIR and FTIR Spectra with exogenous lipids in algal biomass. Bioenergy Res. 4, 22–35. https://doi.org/10.1007/S12155-010-9098-Y/FIGURES/9.

Ma, C., Tan, C., Xie, J., Yuan, F., Tao, H., Guo, L., Cui, B., Yuan, C., Gao, W., Zou, F., Wu, Z., Liu, P., Lu, L., 2023. Effects of different ratios of mannitol to sorbitol on the functional properties of sweet potato starch films. Int. J. Biol. Macromol. 242, 124914. https://doi.org/10.1016/J.IJBIOMAC.2023.124914.

Mendes, J.F., Paschoalin, R.T., Carmona, V.B., Sena Neto, A.R., Marques, A.C.P., Marconcini, J.M., Mattoso, L.H.C., Medeiros, E.S., Oliveira, J.E., 2016. Biodegradable polymer blends based on corn starch and thermoplastic chitosan processed by extrusion. Carbohydr. Polym. 137, 452–458. https://doi.org/10.1016/J.CARBPOL.2015.10.093.

Mittal, R., Ranade, V., 2023. Bioactives from microalgae: A review on process intensification using hydrodynamic cavitation. J. Appl. Phycol. 2023 353 35, 1129–1161. https://doi.org/10.1007/S10811-023-02945-W.

Munaro, D., Mazo, C.H., Bauer, C.M., da Silva Gomes, L., Teodoro, E.B., Mazzarino, L., da Rocha Veleirinho, M.B., Moura e Silva, S., Maraschin, M., 2024. A novel biostimulant from chitosan nanoparticles and microalgae-based protein hydrolysate: Improving crop performance in tomato. Sci. Hortic. (Amsterdam). 323, 112491. https://doi.org/10.1016/J.SCIENTA.2023.112491.

Nitsos, C., Filali, R., Taidi, B., Lemaire, J., 2020. Current and novel approaches to downstream processing of microalgae: a review. Biotechnol. Adv. 45, 107650. https://doi.org/10.1016/j.biotechadv.2020.107650.

Perdana, M.I., Ruamcharoen, J., Panphon, S., Leelakriangsak, M., 2021. Antimicrobial activity and physical properties of starch/chitosan film incorporated with lemongrass essential oil and its application. LWT 141, 110934. https://doi.org/10.1016/J.LWT.2021.110934.

Ramalho, E.X., de Castro, R.J.S., 2023. Covalent bonding immobilization of a Bacillus licheniformis protease on chitosan and its application in protein hydrolysis. Biocatal. Agric. Biotechnol. 50, 102713. https://doi.org/10.1016/J.BCAB.2023.102713.

Ren, F., Wang, J., Yu, J., Zhong, C., Xie, F., Wang, S., 2021. Dissolution of Cellulose in Ionic Liquid-DMSO Mixtures: Roles of DMSO/IL Ratio and the Cation Alkyl Chain Length. ACS Omega 6, 27225–27232. https://doi.org/10.1021/ACSOMEGA.1C03954/ASSET/IMAGES/MEDIUM/AO1C03954_M001.GIF.

Rojo, E.M., Piedra, I., González, A.M., Vega, M., Bolado, S., 2021. Effect of process parameters on the valorization of components from microalgal and microalgal-bacteria biomass by enzymatic hydrolysis. Bioresour. Technol. 335, 125256. https://doi.org/10.1016/J.BIORTECH.2021.125256.

Romano, S., De Santis, S., Martinelli, A., Rocchi, L.A., Rocco, D., Sotgiu, G., Orsini, M., 2023. Starch Films Plasticized by Imidazolium-Based Ionic Liquids: effect of Mono- and Dicationic Structures and Different Anions. ACS Appl. Polym. Mater. 5, 8859–8868. https://doi.org/10.1021/ACSAPM.3C01235/ASSET/IMAGES/LARGE/AP3C01235_0006.JPEG.

Sari, Y.W., Bruins, M.E., Sanders, J.P.M., 2013. Enzyme assisted protein extraction from rapeseed, soybean, and microalgae meals. Ind. Crops Prod. 43, 78–83. https://doi.org/10.1016/j.indcrop.2012.07.014.

Schmitz, S., Dona, A.C., Castignolles, P., Gilbert, R.G., Gaborieau, M., 2009. Assessment of the Extent of Starch Dissolution in Dimethyl Sulfoxide by 1H NMR Spectroscopy. Macromol. Biosci. 9, 506–514. https://doi.org/10.1002/MABI.200800244.

Seymour, R.B., Johnson, E.L., 1976. The effect of solution variables on the solution of cellulose in dimethyl sulfoxide. J. Appl. Polym. Sci. 20, 3425–3429. https://doi.org/10.1002/APP.1976.070201220.

Stuart, B.H., 2005. Infrared Spectroscopy: fundamentals and Applications. Infrared Spectrosc. Fundam. Appl. 1–224. https://doi.org/10.1002/0470011149.

Suarez Ruiz, C.A., Baca, S.Z., van den Broek, L.A.M., van den Berg, C., Wijffels, R.H., Eppink, M.H.M., 2020a. Selective fractionation of free glucose and starch from microalgae using aqueous two-phase systems. Algal Res. 46, 101801. https://doi.org/10.1016/j.algal.2020.101801.

Suarez Ruiz, C.A., Kwaijtaal, J., Peinado, O.C., Van Den Berg, C., Wijffels, R.H., Eppink, M.H.M., 2020b. Multistep Fractionation of Microalgal Biomolecules Using Selective Aqueous Two-Phase Systems. ACS Sustain. Chem. Eng. 8, 2441–2452. https://doi.org/10.1021/acssuschemeng.9b06379.

Tedeschi, A.M., Di Caprio, F., Piozzi, A., Pagnanelli, F., Francolini, I., 2021. Sustainable Bioactive Packaging Based on Thermoplastic Starch and Microalgae. Int. J. Mol. Sci. 2022, Vol. 23, Page 178 23, 178. https://doi.org/10.3390/IJMS23010178.

Theophanides, T., Theophanides, T., 2012. Infrared Spectroscopy - Materials Science, Engineering and Technology. Infrared Spectrosc. - Mater. Sci. Eng. Technol. https://doi.org/10.5772/2055.

Vilpoux, O.F., Santos Silveira Junior, J.F., 2023. Global production and use of starch. Starchy Crop. Morphol. Extr. Prop. Appl. 43–66. https://doi.org/10.1016/B978-0-323-90058-4.00014-1.

Wang, Y., Ho, S.H., Cheng, C.L., Guo, W.Q., Nagarajan, D., Ren, N.Q., Lee, D.J., Chang, J. S., 2016. Perspectives on the feasibility of using microalgae for industrial wastewater treatment. Bioresour. Technol. 222, 485–497. https://doi.org/10.1016/J.BIORTECH.2016.09.106.

Zawadzki, J., Kaczmarek, H., 2010. Thermal treatment of chitosan in various conditions. Carbohydr. Polym. 80, 394–400. https://doi.org/10.1016/J.CARBPOL.2009.11.037.

Zhang, X., Davidson, E.A., Mauzerall, D.L., Searchinger, T.D., Dumas, P., Shen, Y., 2015. Managing nitrogen for sustainable development. Nat. 2015 5287580 528, 51–59. https://doi.org/10.1038/nature15743.